Unipolar Atrial Electrogram Morphology from an Epicardial and Endocardial Perspective

Lisette van der Does
Paul Knops
Christophe Teuwen
Corina Serban
Roeliene Starreveld
Eva Lanters
Elisabeth Mouws
Charles Kik
Ad Bogers
Natasja de Groot

ABSTRACT

Background: Endo-epicardial asynchrony (EEA) and the interplay between the endocardial and epicardial layers could be important in the pathophysiology of atrial arrhythmias. The morphological differences between epicardial and endocardial atrial electrograms have not yet been described, and electrogram morphology may hold information about the presence of EEA. The purpose of this study was to directly compare epicardial to endocardial unipolar electrogram morphology during sinus rhythm (SR) and to evaluate whether EEA contributes to electrogram fractionation by correlating fractionation to spatial activation patterns.

Methods: In 26 patients undergoing cardiac surgery, unipolar electrograms were simultaneously recorded from the epicardium and endocardium at the inferior, middle and superior right atrial (RA) free wall during SR. Potentials were analyzed for epi-endocardial differences in local activation time, voltage, RS ratio and fractionation. The surrounding and opposite electrograms of fractionated deflections were evaluated for corresponding local activation times in order to determine whether fractionation originated from EEA.

Results: The superior RA was predisposed for delayed activation, EEA and fractionation. Both epicardial and endocardial electrograms demonstrated an S-predominance. Fractionation was mostly similar between the two sides; however, incidentally deflections up to 4 mV on one side could be absent on the other side. Remote activation was responsible for most fractionated deflections (95%) in SR, of which 4% could be attributed to EEA.

Conclusion: Local epi-endocardial differences in electrogram fractionation occur occasionally during SR but will likely increase during arrhythmias due to increasing EEA and (functional) conduction disorders. Electrogram fractionation can originate from EEA and this study demonstrated that unipolar electrogram fractionation can potentially identify EEA.

INTRODUCTION

Differences in electrophysiological properties of the ventricular epicardial and endocardial wall have been long recognized and linked to arrhythmogenesis.[1] Although wavefronts traveling out of sync at the epicardium and endocardium of the thin atrial wall were already demonstrated more than two decades ago,[2] unravelling of the link between endo-epicardial asynchrony (EEA) and atrial arrhythmias only started recently.[3] Asynchrony in epicardial versus endocardial propagating waves and the complex fiber arrangement of the atria may also give rise to epi-endocardial differences in the morphology of electrograms. Houben et al. have proposed that the ratio between the R-peak and S-peak of unipolar atrial electrograms may differ between the epicardium and endocardium and could identify the leading layer.[4] Other features of electrogram morphology such as amplitude and fractionation have been used to identify areas with scar tissue and arrhythmogenic areas.[5] Electrogram fractionation occurs when inhomogeneity in conduction occurs within or remotely from the recording site and can have structural or functional causes.[6] The intricate structure of the atria might be a substrate for epi-endocardial differences in fractionation and occurrence of EEA. Asynchronous activation within the wall could in turn be responsible for additional deflections in electrograms.

In a clinical setting, epicardial and endocardial mapping is never performed simultaneously; therefore, the differences and relationships between epi- and endocardial atrial electrogram morphology are so far unknown. This study is the first to directly compare unipolar epicardial electrograms to endocardial electrograms that were recorded simultaneously at the right atrial wall during sinus rhythm (SR) in order to evaluate whether 1) (local) morphological features differ between epicardial and endocardial electrograms and 2) a fractionated electrogram morphology can arise from local EEA in activation. To this end, we developed a method to classify fractionation to its electrophysiological origin by correlating fractionated potentials to spatial patterns of activation.

METHODS

Study population

Twenty-six adult patients undergoing first-time cardiac surgery with use of cardiopulmonary bypass were included (21 male; age 67±10 years). Nineteen patients (73%) were operated for coronary artery disease, 12 (46%) for (concomitant) valvular heart disease, 11 (42%) patients had a history of atrial fibrillation (AF), and 6 (23%) had impaired left ventricular function. Clinical characteristics are described in detail in Supplemental Table 1. The study protocol was approved by the local ethics committee (MEC2015-373) and all patients provided informed consent for inclusion before surgery.

Intraoperative endo-epicardial mapping

Two multi-electrode arrays, each containing 128 electrodes with 2 mm interelectrode spacing, were fixed on spatulas and positioned directly opposite to each other (Figure 1, left panel). After arterial cannulation for cardiopulmonary bypass, an incision was made in the RA appendage for venous cannulation. Before venous cannulation, one spatula was introduced in the right atrium through the incision and the opening around the spatula was closed with a purse-string suture.[7] Atrial epicardial and endocardial unipolar electrograms were simultaneously recorded for 5-10 seconds during SR at three different locations of the RA free wall: 1) inferior RA, 2) mid-RA, 3) superior RA. Unipolar electrograms were sampled at 1 kHz and stored on hard disk after amplification, filtering (0.5-500 Hz) and analogue-to-digital conversion. Detailed methods are provided in the Supplemental Material.

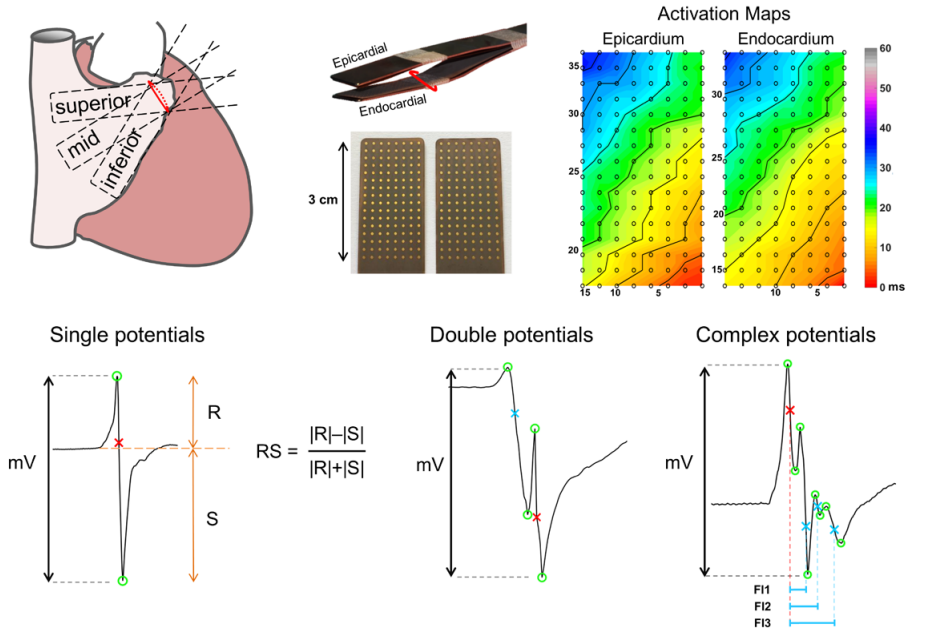

Figure 1. Endo-epicardial mapping and signal analyses.
Left: Two spatulas with 128-electrode arrays are fixed together and one spatula is introduced in the right atrium through the incision for venous cannulation. Unipolar electrogram recordings are made on 3 locations: towards the inferior vena cava (inferior RA), the superior vena cava (superior RA) and in between, towards the terminal crest (mid-RA). Middle: the steepest deflection is marked as local activation time (AT, red cross) and additional deflections (blue crosses) are marked as fractionated deflections if the criteria for fractionation are met (see text). Signal morphology is analyzed for number of deflections, the RS-ratio (only single potentials) and peak-to-peak amplitude (potentials with multiple deflections: amplitude between the maximal and minimal peak). Fractionation interval (FI) is the time between the fractionated deflection and local AT within the potential. Right: An example of epi-endocardial activation time maps with isochrones are shown on the top. For classification, two rings of electrograms around a fractionated deflection (blue dot) in the same and opposite plane are searched for coinciding (peak-to-peak time distance ±3 ms error margin) deflections of local ATs.

Data analysis

Electrogram morphology was analyzed semi-automatically in MATLAB R2016a (The MathWorks Inc., Natick, MA). Electrograms with injury potentials were excluded from analysis and recording sites with ≥25% excluded or missing electrograms were excluded in total (Supplemental Figure 1). SR potentials were analyzed for fractionation (number of deflections), peak-to-peak amplitude (voltage) and RS ratios; atrial extrasystoles were excluded. The potentials in each electrogram were averaged for voltage and RS ratio comparison. The steepest negative deflection of a potential was marked as local activation time (AT) if the slope was ≥0.05 mV/ms and the deflection had a signal-to-noise ratio >2. Additional deflections with a slope ≥10% of the local AT (and ≥0.05 mV/ms), peak-to-noise ratio >2, and either an amplitude >1/6 of the amplitude of the local activation deflection or a signal-to-noise ratio >5 were marked as fractionation (Supplemental Figure 2). Only nonfractionated potentials (single deflections) were analyzed for the ratio between the R-peak and S-peak (RS ratio).[4] All signal markings were manually checked and corrected in case of markings on electrical artifacts evaluated by a consensus of two investigators. Figure 1 shows the analysis of signal amplitudes and RS ratios. Delayed activation is defined as interelectrode differences in AT >11 ms (<17 cm/s) of electrodes in the *same* plane. The amount of delayed activation is expressed in millimeters: number of interelectrode differences >11 ms × interelectrode distance (2 mm).

Analysis of local epi-endocardial differences

Local differences in AT, RS ratio and fractionation between the epicardium and endocardium were determined by comparing each electrogram with the electrograms in the opposite square: the exact opposite electrogram and its 8 surrounding electrograms. The local difference was the minimal difference of the potentials in the opposite square, as previously described.[3] Border electrodes were excluded from analysis of local differences. For local differences in RS ratio, only recordings with <25% fractionated potentials were included. Fractionated potentials with ≥15 ms between the first and last deflections were analyzed for detection of all (separate) deflections on both sides at the same time (epi-endocardial comparison of coinciding deflections). Each deflection was tested whether its steepest point fell within peak-to-peak time limits (±3 ms error margin) of deflections at the opposite square. The deflections that were not detected on the other side, as no coinciding deflection meeting the annotation criteria was present, were also manually examined for visual absence.

Classification of fractionation

Each fractionated deflection was evaluated if it could be attributed to remote activation, that is, to delayed (discontinuous) activation in the surrounding tissue in the *same* layer or to EEA. The adjacent and opposite, first and second electrode rings around the fraction-

ated potential were searched for deflections of local ATs coinciding with the fractionated deflection. If the fractionated deflection fell within peak-to-peak time limits (±3 ms) of the deflections of local ATs, it was classified based on the plane(s) where the corresponding local AT(s) was located (Figure 1, right panel). Corresponding ATs were present in either 1) the same plane, 2) the opposite plane, 3) both planes or 4) none of the planes (absence of corresponding local AT). Border electrodes were excluded from analysis. Fractionation interval for fractionated deflections was defined as the time interval between the fractionated deflection and the deflection of the local AT (Figure 1, middle panel).

Statistical analysis

Normally distributed data are given as mean±SD and skewed data are given as median (p10-p90). Electrophysiological parameters were in square root or log-transformed in case of a non-normal distribution. Linear mixed models were used to investigate the associations between location (independent variable) and electrophysiological parameters (dependent variable). Random intercepts were used for location. When normal distributions could not be obtained using transformations, the Friedman test was used to investigate the associations. Comparison of epicardial and endocardial amounts of delayed activation was done with the Wilcoxon signed rank test. Spearman rho coefficient was used to determine the correlation between cycle length and amount of delayed activation.

The associations of location and side with morphological parameters of electrograms were evaluated using Generalized Estimated Equations. The skewed distribution of RS ratios could not be transformed to a normal distribution; therefore, RS ratios were converted to a binomial distribution by setting the lowest-quartile (<-0.51) of RS values as “highly” S-dominant. Correlation structure was chosen based on the goodness of fit in the guasi-likelihood function and the inferior RA served as the reference in the models evaluating locations. Statistical analyses were performed using IBM SPSS Statistics version 21 (IBM corp.,Armonk, NY).

RESULTS

Electrophysiological data and parameters

Recordings at the inferior, mid and superior RA of 26, 25 and 21 patients, respectively, were included. SR cycle lengths did not change between the RA locations; inferior 902±202, mid 908±193 (P=0.72) and superior 827±162 (P=0.17). The amount of delayed activation increased from the inferior to the superior RA: 12 (0-80) mm, 32 (0-99) mm (P=0.095), 74 (18-178) mm (P<0.001). At the superior RA, the endocardium demonstrated more delayed activation than the epicardium; 26 (0-61) mm vs. 44 (7-124) mm (P=0.010). No correlation

was present between SR cycle length and amount of delayed activation (r=0.05, *P*=0.81). A total of 102,129 potentials were analyzed in 16,954 electrograms, including 50,714 potentials of 8423 electrograms recorded at the epicardium and 51,415 potentials of 8531 electrograms recorded at the endocardium. An overview of the individual patient results is provided in Supplemental Table 2.

Unipolar voltages

From the inferior to the middle and superior RA, electrogram voltage decreased gradually from 8.0 (3.1-16.3) mV, to 6.4 (2.4-13.3) mV (*P*=0.001) and to 4.9 (1.7-11.7) mV (*P*<0.001). Opposite epicardial and endocardial electrogram amplitudes demonstrated a positive linear relationship (Figure 2, bottom left panel). Because it was expected that voltage is dependent on fractionation, potentials were categorized into singles, doubles and complex fractionated (>2 deflections) potentials. Figure 2 shows that unipolar voltage indeed decreased with more fractionated potentials at both the epicardium and endocardium. The largest epi-endocardial difference in amplitude was observed for unipolar potentials with single deflections that had an epicardial vs endocardial amplitude of respectively 8.3 (3.8-14.7) mV vs 6.7 (2.8-16.1) mV (*P*=0.08). Double potentials had epi-endocardial amplitudes of 4.1 (1.6-8.3) mV vs 3.8 (1.3-8.5) mV (*P*=0.45). Complex fractionated potentials had amplitudes of 2.5 (1.1-4.7) mV vs 2.7 (1.2-5.1) mV (*P*=0.08). The percentile ranges of endocardial potentials were wider than of epicardial potentials.

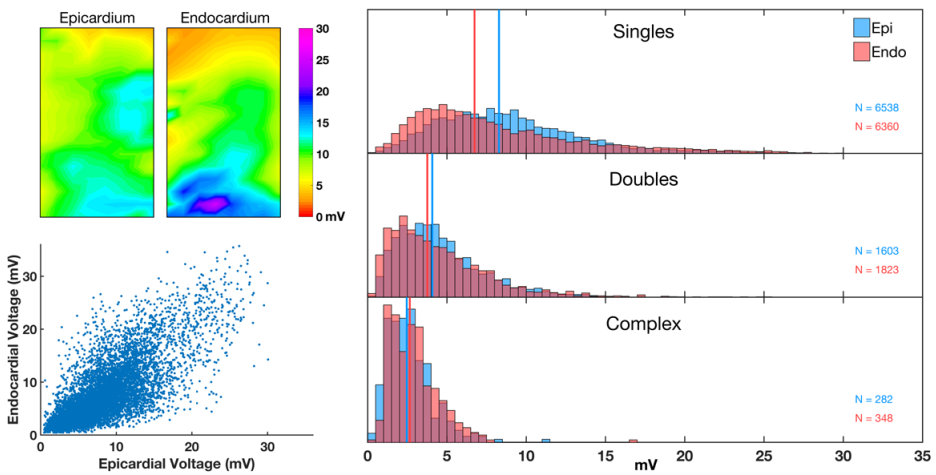

Figure 2. Epi-endocardial unipolar voltage.
Top left: Example of epicardial and endocardial voltage maps. Bottom left: Scatter plot of epi-endocardial unipolar voltages. Right: Relative frequency histograms of unipolar epicardial and endocardial electrogram voltage for singles, doubles and complex fractionated potentials. Vertical lines indicate the median.

RS ratio of epi-endocardial single deflections

The RS ratios of potentials with single deflections recorded at the epicardium and endocardium are shown in Figure 3 for each RA location. Both sides demonstrated a clear S-predominance, which increased at the mid-RA (*P*=0.001) and superior RA (*P*<0.001). Epicardial vs endocardial median RS ratios at the inferior RA were -0.23 (-0.53 to +0.26) vs. -0.25 (-0.53 to +0.26); at the mid-RA were -0.32 (-0.78 to +0.06) vs. -0.34 (-0.72 to +0.07); and at the superior RA were -0.43 (-0.96 to +0.09) vs. -0.46 (-0.97 to +0.11). Many potentials at the superior RA, the area of the sinus node, had an S-morphology (RS ratio of -1) at both sides (11% vs 13%). Local differences in RS ratios were between 0 and 0.22 for 95% of the data, without either side having more S-predominance than the other side (Figure 3).

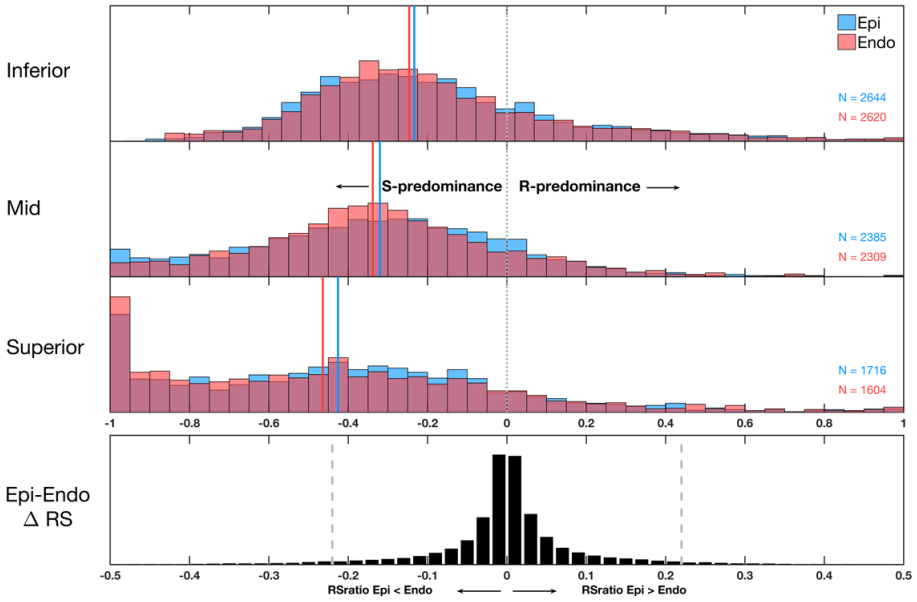

Figure 3. Relative frequency histograms of epicardial and endocardial RS-ratios and local epi-endocardial RS differences.

Top 3 panels: RS-ratios per location, negative values represent increasing S-predominance, positive values represent increasing R-predominance. Medians are indicated by vertical colored lines. Bottom panel: local differences in RS-ratio between epicardium and endocardium. Negative values represent smaller RS-ratio values at the epicardium, positive values represent smaller RS-ratio values at the endocardium. Between the dashed grey lines 95% of the data is represented.

Epi-endocardial differences in fractionation

Relative incidence of singles, doubles, triples and potentials with >3 deflections was 76%, 20%, 3% and <1%, respectively. The incidence of fractionated potentials (>1 deflection) showed an increasing trend from the inferior RA (16%) towards the mid-RA (22%, *P*=0.136) and was highest at the superior RA (36%, *P*<0.001). Epicardial vs endocardial incidence of

fractionation at the inferior RA was 15% vs 17% (*P*=0.29), at the mid-RA was 21% vs. 22% (*P*=0.45), and the superior-RA demonstrated a trend towards more fractionated potentials at the endocardium: 33% vs. 38% (*P*=0.09). Local epi-endocardial differences in the number of detected deflections occurred in 6.6% (Table 1).

Table 1. Epicardial vs. endocardial fractionation

	Total fractionation (%)								Local differences in fractionation Δ Epi-endo no. of deflections (%)			
	Singles		Doubles		Triples		Complex(>3)					
	Epi	Endo	Epi	Endo	Epi	Endo	Epi	Endo	0	1	2	3>
Inferior	84.7	82.9	12.8	14.5	2.3	2.4	0.2	0.2	95.7	4.1	0.2	<0.1
Mid	79.4	77.7	17.5	19.2	2.6	2.8	0.4	0.3	93.2	6.5	0.2	<0.1
Superior	67.3	62.0	27.1	30.6	4.4	6.4	1.2	1.1	90.8	8.7	0.5	<0.1
Total	77.8	75.0	18.6	20.8	3.0	3.7	0.6	0.5	93.4	6.3	0.3	<0.1

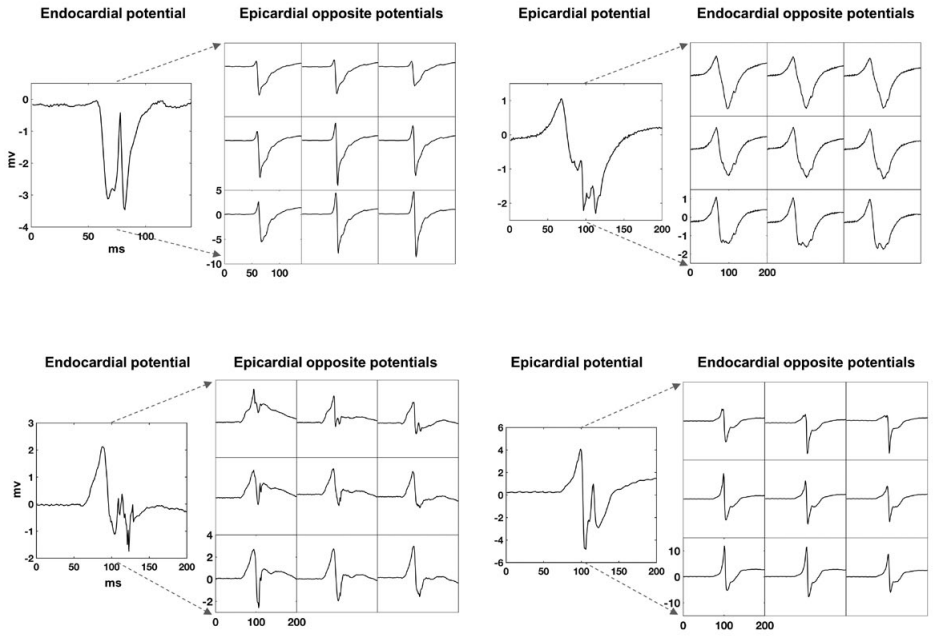

Figure 4. Examples of local differences in fractionation between epicardium and endocardium.
Four fractionated potentials are shown recorded at the epicardium or endocardium with the nine electrograms on the direct opposite side (direct opposite and its 8 surrounding electrograms). In the lower right example the second deflection of 4mV at the epicardium is totally absent at the endocardium.

A total of 1580 electrograms contained potentials with fractionated deflections having a fractionation interval ≥15 ms. In 271 of those 1580 cases, deflections remained undetected on the other side, based on the annotation criteria, and 53 of those 271 deflections were also visually completely absent. In 41 of 271 cases, the same number of deflections were present on both sides but with epi-endocardial time-differences between the corresponding deflections of 4-85 ms (median 13 ms). In the remaining 177 of 271 cases, a (small) deflection was visually observed that did not meet the criteria for a deflection. Examples of epi-endocardial differences in fractionation (Figure 4) demonstrate that deflections up to a maximum of 4 mV on one side could be absent at that location on the other side.

Endo-epicardial asynchrony during sinus rhythm

Right atrial EEA >14 ms, as previously defined for AF[3], occurred at the inferior RA in 12% of the patients, at the mid-RA in 19% and at the superior RA in 57%. EEA increased from the inferior to the superior RA (*P*=0.001). One patient had by far the most EEA of the study group (44.4% at the mid-RA) with an endocardial delay of >50 ms. EEA during SR is mainly determined by one side being delayed. The degree and incidence of EEA are provided in Supplemental Figure 3.

Fractionation attributable to delayed activation or endo-epicardial asynchrony

For the far majority (95%) of fractionated deflections, a corresponding local AT was present in the surrounding tissue of the same or opposite layer (Table 2). In 4%, a local AT was only observed in the *opposite* plane, which corresponds to sites with EEA (Figure 5A). In 9%, a corresponding local AT was only observed in the *same* plane, which corresponded to a site with delayed activation that was asymmetrical between the epicardium and endocardium (local delayed activation in one plane) (blue outlined potential, Figure 5B). In 83% of fractionated deflections, a matching local AT was present in both planes. This group contains 3 underlying causes: 1) symmetrical epi-endocardial delayed activation (Figure 5C), 2) asymmetrical epi-endocardial delayed activation; after the site with a delay in activation (Figure 5B), 3) short fractionation intervals (Figure 5C). Most can be attributed

Table 2. Classification of fractionated deflections corresponding with local activation times

	Doubles				Triples				Complex (>3)				Total
	N	%	FI (ms)		N	%	FI (ms)		N	%	FI (ms)		N (%)
Same plane	144	7	28	(14-58)	73	11	22	(10-27)	24	15	13	(11-47)	241 (9)
Opposite plane	69	3	27	(11-60)	26	4	26	(16-37)	8	5	38	(22-38)	103 (4)
Both planes	1682	85	12	(8-24)	553	82	12	(8-23)	99	63	14	(9-39)	2334 (83)
None	91	5	32	(17-60)	22	3	30	(18-56)	27	17	35	(21-35)	140 (5)

FI = fractionation interval.

to short fractionation intervals as the median fractionated interval for these deflections was only 12 ms (Table 2). For the remaining 5% of fractionated deflections, no matching local AT was found. Some of those had corresponding local ATs distanced >4 mm of the fractionated site (Figure 5B), and more than half (61%) were deflections on electrodes that did not have a complete second ring to search for corresponding ATs (relative border electrodes). Figure 5D shows an example of a fractionated deflection likely reflecting intramural inhomogeneity in conduction; it only appears in center electrodes without any corresponding local AT. Potentials with >3 deflections most often had deflections without any corresponding local AT compared to doubles and singles (17% vs 3% and 5%).

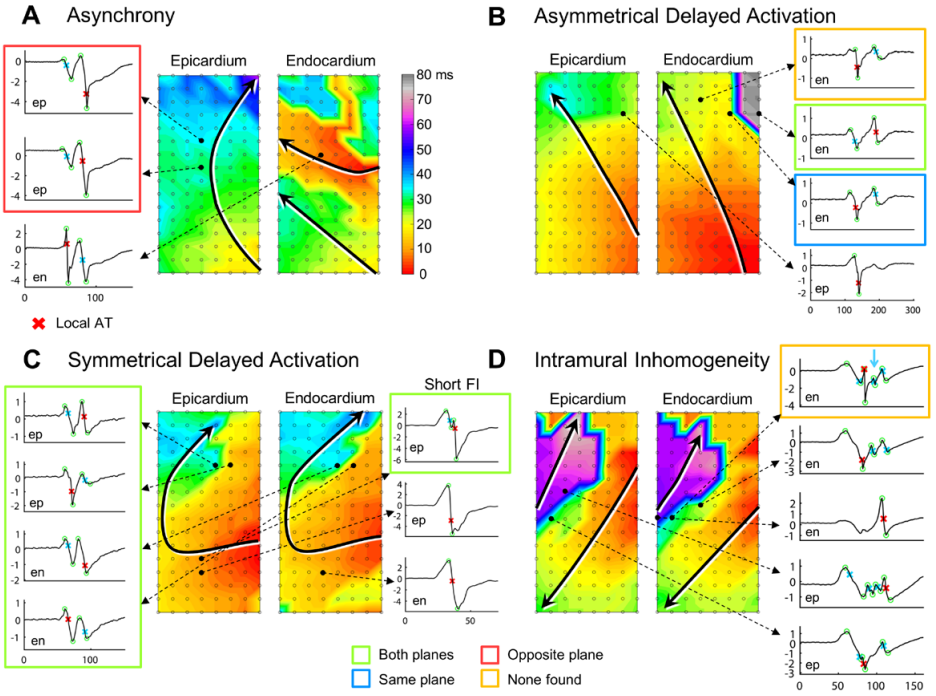

Figure 5. Fractionated potentials attributable to various patterns of conduction disorders.
Panels A-D demonstrate examples where fractionated potentials correspond to remote myocardial activation in the same plane (outlined in blue), in the opposite plane (outlined in red) or in both planes (outlined in green) or do not correspond with any remote activation (outlined in orange). A: Endo-epicardial asynchrony causes fractionated deflections (blue marked deflections) at the epicardium, matching local activation times (AT, red marked deflections) are only present in the opposite plane. B: At sites with asymmetrical delayed activation (DA), fractionated deflections in front of an area of DA correspond to local ATs in the same plane, however at the delayed site, fractionated deflections correspond to ATs in both planes. In some cases, even sites >4 mm of the DA site show corresponding fractionated potentials. C: Fractionated deflections at sites with symmetrical DA at both sides, local ATs are present in both planes. Deflections with short fractionation intervals (FI) similar to normal conduction velocity will also mostly have matching local ATs at both sides. D: The third deflection of the upper complex fractionated potential does not correspond to any local AT in the same or opposite plane, demonstrating intramural inhomogeneity in conduction.

DISCUSSION

Electrogram morphology is often used for the identification of structural or electrical remodeled areas with arrhythmogenic properties. In most settings, electroanatomical mapping is performed via endovascular catheters at the endocardial side. In recent perspective, it has become clear that asynchrony within the atrial wall can have an important role in the mechanism of atrial arrhythmias.[3,8] Our study has shown that EEA >50 ms can already be present during SR and that unipolar electrogram fractionation can represent the presence of EEA. However, electrical activity within or on the opposite side of the atrial wall can also occasionally be missed when electrograms are recorded only from one side of the wall. At the superior RA, the highest amount of delayed activation and EEA was observed and resulted, because of their interdependence, in the highest amount of fractionated electrograms and the lowest voltages.

Right atrial anatomy

Variations between epi- and endocardial unipolar voltage can be explained from the anatomical structure of the RA wall. The surface of the endocardial RA appendage, unlike the smooth epicardial side, is very irregular due to the pectinate muscles of varying diameters and the thick terminal crest. The mass of cardiac bundles is positively correlated to unipolar electrogram voltage and anatomical studies have shown that pectinate muscles can vary from <1 to 7 mm.[9,10] The different sizes and arrangement of the bundles also cause a variation in the level of contact with the electrodes on the flat array. Our high-resolution epicardial mapping study demonstrated recently that epicardial breakthrough waves during SR were most frequently observed at the superior RA.[11] EEA indeed occurred most often in this area which also correlated to the highest amount of delayed activation and fractionation. The superior RA contains the sinus node within its fibrous case and the thickest part of the anisotropic terminal crest, which may underlie the proneness of this area to delays in activation, EEA and breakthrough waves.[9,12] The structural variability of the RA therefore influences epi-endocardial synchronicity and electrogram morphology. Electrical activity that remains undetected on one side may relate to thicker or more irregular parts of the RA.

The value of unipolar electrograms

Unipolar electrograms have the benefit over bipolar electrograms that their morphology carries additional information about the progression of the wavefront and remote activations. The ratio between the positive and negative component of a unipolar electrogram characterizes the start or end of a wavefront and possibly the curvature of the wavefront and conduction velocity.[13] Epicardial electrograms recorded during AF demonstrated an S-predominance which could not be strongly correlated to wavefront curvature or

anisotropy.[4] A tilted transmural stance of the wavefront resulting in an epicardial lead with constant epicardial to endocardial activation was proposed as theoretical explanation for S-predominance during AF which would present with more R-predominance at the endocardium. In this study, both epicardial and endocardial electrograms showed an S-predominance and endocardial electrograms did not have higher RS ratios than epicardial electrograms. Therefore, S-predominance during SR cannot be explained by epicardial to endocardial activation or vice versa. Previous studies demonstrated that endocardial unipolar electrogram voltage is more useful for detecting areas of scar at the epicardium than bipolar electrogram voltage because of their range of view.[14] We established that the view of unipolar electrograms can signify the presence of EEA and can reveal areas with intramural inhomogeneous conduction. Detecting EEA from the endocardium alone requires the atrial "farfield" potentials on unipolar electrograms that will be filtered out with standard bipolar recordings. Furthermore, the limitations of registering all atrial activity from throughout the atrial wall demonstrated by our high-density contact mapping approach will only increase with noncontact mapping systems. Therefore, current mapping approaches may be insufficient to detect transmural atrial activity.

Epi-endocardial electrograms during atrial arrhythmias

The incidence of local differences in epicardial and endocardial electrogram morphology and of electrogram fractionation due to EEA is relatively low during SR. According to the observations of Schuessler et al., epi-endocardial differences in activation were least prominent during SR and high-rate pacing, but were significantly increased with premature stimulation.[2] In a goat model of AF, the amount of EEA increased with AF persistence, which was also associated with more inhomogeneous conduction patterns and a shortening of fibrillation cycle length.[15] Our previous study in humans also demonstrated more EEA at the RA wall during AF with incidences between 0.9 and 55.9%.[3] EEA occurs more frequently in atrial arrhythmias because of the increase of inhomogeneous conduction and (functional) conduction disorders. Therefore, fractionation due to EEA and local differences in epi-endocardial electrogram fractionation are expected to increase during atrial arrhythmias. The RA appendage, which has the thickest wall of the whole atria, is especially susceptible to local differences in electrogram morphology and EEA. Nevertheless, breakthrough waves also occur frequently at the left atrium, indicating the presence of EEA, and with wavefronts decreasing in size during AF, electrogram amplitude will decrease causing local differences in fractionation more likely to occur in any area.[11,16] When fractionated electrograms are ablated only from the endocardial side, epicardial fractionated sites could be overlooked. However, more importantly, these fractionated sites have different pathophysiological origins, including EEA, and ablating all fractionated electrograms would only increase needless atrial scarring.

Study limitations

Intraoperative simultaneous endo-epicardial mapping in living humans can only be safely performed at the RA; therefore, we could not evaluate the relation of epicardial and endocardial electrograms at the structurally less complicated left atrium. However, epicardial breakthroughs also are often present at the left atrium, indicating the occurrence of EEA at the left atrium during SR as well.[11] The finite area of the mapping array and relatively low incidence of (complex) fractionation during SR limited the classification of fractionated deflections to those situated in the center of the array. The relatively small number of fractionated deflections classified to no corresponding local AT is probably still an overestimation.

CONCLUSIONS

In SR, EEA of the RA free wall occurs at >50 ms difference between epicardium and endocardium, which has never been described before. Electrograms on both sides demonstrate an S-predominance and the RS ratio cannot be used to identify the leading layer during SR. Fractionated potentials are not always identical on a high-resolution scale and can have local mismatches; however, these mismatches occur in a minority of cases. If a potential is fractionated during SR, most additional deflections can be explained by conduction disorders in the *same* plane and in a small percentage they represent EEA. The incidence of EEA and EEA-based fractionation is relatively low during SR, as was expected. However, during atrial arrhythmias the presence of (functional) conduction disorders and EEA will increase; therefore, epi-endocardial differences in electrogram morphology and EEA-based fractionation will likely increase as well. Particularly interesting, especially for clinical practice, is the observation that the morphology of unipolar electrograms can potentially be a tool to identify areas of EEA when electrograms are recorded on only one side of the wall.

REFERENCES

1. Lukas A, Antzelevitch C. Differences in the electrophysiological response of canine ventricular epicardium and endocardium to ischemia. Role of the transient outward current. Circulation. 1993;88:2903-2915.
2. Schuessler RB, Kawamoto T, Hand DE, Mitsuno M, Bromberg BI, Cox JL, Boineau JP. Simultaneous epicardial and endocardial activation sequence mapping in the isolated canine right atrium. Circulation. 1993;88:250-263.
3. de Groot N, van der Does L, Yaksh A, Lanters E, Teuwen C, Knops P, van de Woestijne P, Bekkers J, Kik C, Bogers A, Allessie M. Direct Proof of Endo-Epicardial Asynchrony of the Atrial Wall During Atrial Fibrillation in Humans. Circ Arrhythm Electrophysiol. 2016;9:e003648.
4. Houben RP, de Groot NM, Smeets JL, Becker AE, Lindemans FW, Allessie MA. S-wave predominance of epicardial electrograms during atrial fibrillation in humans: indirect evidence for a role of the thin subepicardial layer. Heart Rhythm. 2004;1:639-647.
5. Nademanee K, McKenzie J, Kosar E, Schwab M, Sunsaneewitayakul B, Vasavakul T, Khunnawat C, Ngarmukos T. A new approach for catheter ablation of atrial fibrillation: mapping of the electrophysiologic substrate. J Am Coll Cardiol. 2004;43:2044-2053.
6. van der Does LJ, de Groot NM. Inhomogeneity and complexity in defining fractionated electrograms. Heart Rhythm. 2017;14:616-624.
7. Knops P, Kik C, Bogers AJ, de Groot NM. Simultaneous endocardial and epicardial high-resolution mapping of the human right atrial wall. J Thorac Cardiovasc Surg. 2016;152:929-931.
8. Pathik B, Lee G, Sacher F, Haïssaguerre M, Jaïs P, Massoullie G, Derval N, Sanders P, Kistler P, Kalman JM. Epicardial-endocardial breakthrough during stable atrial macroreentry: Evidence from ultra-high-resolution 3-dimensional mapping. Heart Rhythm. 2017;14:1200-1207.
9. Sanchez-Quintana D, Anderson RH, Cabrera JA, Climent V, Martin R, Farre J, Ho SY. The terminal crest: morphological features relevant to electrophysiology. Heart. 2002;88:406-411.
10. Spach MS, Dolber PC. Relating extracellular potentials and their derivatives to anisotropic propagation at a microscopic level in human cardiac muscle. Evidence for electrical uncoupling of side-to-side fiber connections with increasing age. Circ Res. 1986;58:356-371.
11. Mouws E, Lanters E, Teuwen C, van der Does L, Kik C, Knops P, Bekkers J, Bogers A, de Groot N. Epicardial Breakthrough Waves during SR: Depiction of the Arrhythmogenic Substrate? Circ Arrhythm Electrophysiol. 2017:e005145.
12. Fedorov VV, Glukhov AV, Chang R, Kostecki G, Aferol H, Hucker WJ, Wuskell JP, Loew LM, Schuessler RB, Moazami N, Efimov IR. Optical mapping of the isolated coronary-perfused human sinus node. J Am Coll Cardiol. 2010;56:1386-1394.
13. Spach MS, Miller WT, 3rd, Miller-Jones E, Warren RB, Barr RC. Extracellular potentials related to intracellular action potentials during impulse conduction in anisotropic canine cardiac muscle. Circ Res. 1979;45:188-204.
14. Tokuda M, Tedrow UB, Inada K, Reichlin T, Michaud GF, John RM, Epstein LM, Stevenson WG. Direct comparison of adjacent endocardial and epicardial electrograms: implications for substrate mapping. J Am Heart Assoc. 2013;2:e000215.
15. Eckstein J, Zeemering S, Linz D, Maesen B, Verheule S, van Hunnik A, Crijns H, Allessie MA, Schotten U. Transmural conduction is the predominant mechanism of breakthrough during atrial fibrillation: evidence from simultaneous endo-epicardial high-density activation mapping. Circ Arrhythm Electrophysiol. 2013;6:334-341.

16. de Groot NMS, Houben RPM, Smeets JL, Boersma E, Schotten U, Schalij MJ, Crijns H, Allessie MA. Electropathological Substrate of Longstanding Persistent Atrial Fibrillation in Patients With Structural Heart Disease Epicardial Breakthrough. Circulation. 2010;122:1674-1682.

SUPPLEMENTAL MATERIAL CHAPTER 12: DATA ANALYSIS

Patient data inclusion

First activation was required to occur at the top or right atrial side of the mapping area of the superior or middle right atrial recording site, otherwise the rhythm was labelled as an ectopic atrial rhythm and the patient was not included for analysis. Patients required two included recording sites (see below) in order to qualify for study inclusion.

Electrogram exclusion criteria

Electrograms with injury potentials (that can appear due to firm contact with local tissue) were excluded for RS ratio analysis only or excluded for all analyses based on the following criteria:

RS ratio exclusion criteria:	elevation of the baseline after the local potential ≥1/3 and < total amplitude of local potential + concordant shift of potential
Total exclusion criteria:	elevation of the baseline after the local potential ≥1 mV and ≥ total amplitude of local potential

Examples are provided in Supplemental Figure 1.

Recording sites with 25% of missing or total excluded electrograms were excluded from further data analysis which included either a total number of missing/excluded electrograms ≥64 or a total of 32 electrodes from which the exact opposite electrode was missing/excluded. Excluded recording sites of patients are shown in Supplemental Table 2.

Signal marking

Deflections and peaks were marked by the criteria stated in the manuscript using MATLAB R2016a (The MathWorks Inc., Natick, MA). The signal-to-noise ratio was determined by the amplitude of the deflection in relation to the amplitude of the noise (Supplemental Figure 2, top). The peak-prominence of a new peak was used to evaluate the peak-to-noise ratio which defined a new deflection (Supplemental Figure 2, bottom). Noise levels were determined for each electrode separately. All signal markings were checked manually and markings of artifacts were corrected based on a consensus of two investigators.

Analysis of local epi-endocardial differences

Local epi-endocardial differences are analyzed by comparing each potential to the exact opposite potential and its 8 surrounding potentials; 9 potentials in total (=opposite square) and determined by the minimal difference of these 9 comparisons. If the opposite square consisted of 6 or less potentials the electrode was considered a border electrode and was excluded from analysis of local differences.

Supplemental Table 1. Clinical characteristics

Patient no.	Age (yr)	Gender	Structural heart disease	History of AF	RCA S1 stenosis	Dilated RA	Left ventricular function	HT	DM	HC	AAD
1	80	Male	IHD; MVD	Paroxysmal	No	No	Normal	Yes	No	Yes	Class 3
2	71	Male	IHD	None	No	No	Normal	Yes	No	No	Class 2
3	67	Male	IHD	None	Yes	Unknown	Normal	Yes	Yes	No	Class 2
4	70	Male	IHD	None	Yes	Unknown	Normal	Yes	Yes	Yes	Class 2
5	54	Female	IHD	None	No	Unknown	Normal	Yes	Yes	No	-
6	49	Female	IHD; MVD	None	No	Unknown	Mild impairment	No	No	No	-
7	79	Male	IHD; MVD	Persistent	No	Yes	Mild impairment	No	No	No	Class 2, digoxin
8	61	Male	IHD; MVD; PFO	None	No	No	Normal	No	No	No	Class 2
9	73	Male	AVD	None	No	No	Normal	No	No	No	-
10	59	Male	AVD	None	No	Unknown	Normal	Yes	No	No	Class 2
11	68	Male	IHD	Paroxysmal	No	No	Mild impairment	No	No	No	Class 2
12	53	Male	IHD	Paroxysmal	No	Unknown	Normal	No	No	No	Class 2
13	72	Male	IHD	None	No	No	Normal	Yes	Yes	Yes	Class 3
14	64	Female	AVD; MVD	None	No	No	Normal	No	Yes	No	Class 2
15	67	Male	AVD	None	No	Unknown	Normal	Yes	Yes	Yes	-
16	47	Male	IHD	None	No	Unknown	Normal	No	Yes	No	Class 2
17	85	Male	IHD	Paroxysmal	No	Unknown	Normal	Yes	No	No	Class 2, digoxin
18	65	Male	IHD	None	No	Unknown	Normal	Yes	No	No	Class 2
19	53	Male	IHD	Persistent	Yes	Yes	Severe impairment	No	No	No	Class 2, digoxin
20	71	Male	-	Paroxysmal	No	Unknown	Normal	Yes	No	No	Class 2+3
21	71	Male	IHD; MVD	Paroxysmal	Yes	No	Moderate impairment	Yes	No	Yes	Class 1+2
22	64	Male	IHD; AVD	Paroxysmal	No	No	Normal	Yes	No	Yes	Class 2

Supplemental Table 1. Clinical characteristics (continued)

Patient no.	Age (yr)	Gender	Structural heart disease	History of AF	RCA S1 stenosis	Dilated RA	Left ventricular function	HT	DM	HC	AAD
23	76	Female	MVD	Longstanding Persistent	No	Yes	Normal	Yes	Yes	No	Class 2, digoxin
24	64	Female	MVD; TVD	Longstanding Persistent	No	Unknown	Mild impairment	No	No	No	Class 4, digoxin
25	67	Male	IHD	None	No	No	Normal	No	Yes	Yes	Class 2
26	82	Male	IHD	None	No	Unknown	Normal	Yes	Yes	No	Class 2
Total/ mean	67±10	Male 21 (81%)	IHD 19 (73%) VHD 12 (46%)	11 (42%)	4 (15%)	3	Normal 20 (77%)	15 (58%)	10 (39%)	7 (27%)	-

IHD = ischemic heart disease; MVD = mitral valve disease; AVD = aortic valve disease; TVD = triscuspid valve disease; PFO = persistent foramen ovale; VHD = valvular heart disease; AF = atrial fibrillation; RCA S1 = right coronary artery segment 1 (proximal); HT = hypertension; DM = diabetes mellitus; HC = hypercholesterolemia; AAD = antiarrhythmic drugs.

Supplemental Table 2. Individual results of electrophysiological parameters and epi-endocardial electrogram morphology

Patientno.	Location	SRCL (ms)	DA (mm)		Voltage (mV)		RS ratio		Fractionation (%)		EEA (%)	Epi delay (%)	Endo delay (%)
			Epi	Endo	Epi	Endo	Epi	Endo	Epi	Endo			
1	inferior	1047	32	20	9.9	12.5	-0.24	-0.19	17	25	0	0	0
	mid	1171	8	12	7.5	9.5	-0.22	-0.32	16	25	0	0	0
	superior	563	24	36	7.6	7.4	0.19	0.07	35	37	0	0	0
2	inferior	1024	8	12	10.7	12.1	-0.41	-0.43	10	11	0	0	0
	mid	1008	72	36	6.3	6.6	-0.60	-0.61	56	55	6.2	4.6	1.6
	superior						excluded						
3	inferior	998	58	46	5.9	6.6	-0.20	-0.30	49	44	0.2	0	0.2
	mid						excluded						
	superior	1002	50	58	3.3	3.1	0.10	0.14	55	57	0	0	0
4	inferior	1088	2	8	9.5	11.3	-0.28	-0.24	19	12	0	0	0
	mid	1043	34	66	3.9	3.1	-0.80	-0.67	27	49	1.7	1.3	0.5
	superior	840	54	130	4.6	2.8	-0.68	-0.74	34	62	0.5	0.1	0.4
5	inferior	669	0	0	9.1	5.2	-0.47	-0.39	1	0	0	0	0
	mid	672	0	0	8.4	7.1	-0.31	-0.28	12	7	0	0	0
	superior	707	38	50	4.1	1.9	-0.65	-0.97	24	45	10.0	9.2	0.8
6	inferior	717	0	0	10.4	11.4	-0.21	-0.23	0	2	0	0	0
	mid	696	0	4	8.5	7.9	-0.32	-0.41	3	7	0	0	0
	superior	682	0	24	6.1	5.5	-0.76	-0.96	26	29	0.4	0	0.4
7	inferior	1577	8	2	8.9	7.8	-0.18	-0.20	14	11	0	0	0
	mid	1472	2	6	9.1	7.9	-0.17	-0.28	12	12	0	0	0
	superior						excluded						
8	inferior	729	0	0	9.1	7.5	-0.23	-0.17	5	4	0	0	0
	mid	718	8	24	8.9	6.3	-0.26	-0.34	14	19	0	0	0
	superior	705	18	44	7.1	5.9	-0.39	-0.41	23	24	0	0	0
9	inferior	793	22	44	5.9	3.6	-0.14	-0.28	39	49	0	0	0
	mid	793	12	38	6.0	3.9	-0.23	-0.33	39	43	0	0	0
	superior	895	66	68	4.0	3.4	-0.65	-0.87	51	49	2.6	0.3	2.3
10	inferior	895	4	6	11.5	7.6	-0.46	-0.43	12	4	0	0	0
	mid	1004	8	28	7.5	4.4	-0.73	-0.56	19	21	0	0	0
	superior	1005	22	60	4.3	4.1	-0.99	-0.83	36	72	1.5	0.5	1.1
11	inferior	954	0	0	9.7	9.6	-0.24	-0.20	4	5	0	0	0
	mid	1005	6	6	8.7	6.5	-0.26	-0.24	15	12	0	0	0
	superior	970	26	18	6.1	4.8	-0.26	-0.19	33	34	0.8	0	0.8
12	inferior	983	0	0	9.4	14.3	-0.49	-0.44	6	3	0	0	0
	mid	990	38	60	5.1	4.6	-0.63	-0.69	49	49	10.3	10.3	0

Supplemental Table 2. Individual results of electrophysiological parameters and epi-endocardial electrogram morphology (continued)

Patientno.	Location	SRCL (ms)	DA (mm)		Voltage (mV)		RS ratio		Fractionation (%)		EEA (%)	Epi delay (%)	Endo delay (%)
			Epi	Endo	Epi	Endo	Epi	Endo	Epi	Endo			
	superior	975	54	146	3.0	1.9	-0.77	-0.90	49	89	23.1	2.0	21.2
13	inferior	1014	0	22	5.1	6.0	-0.22	-0.18	22	28	0	0	0
	mid	962	14	24	5.7	5.8	0.05	-0.05	17	19	0	0	0
	superior	1005	16	12	4.6	4.6	-0.11	-0.09	32	23	0	0	0
14	inferior	677	36	34	5.7	3.3	0.44	0.44	30	25	2.8	0.0	2.8
	mid	820	24	16	3.7	3.2	-0.52	-0.57	26	11	0	0	0
	superior	689	62	72	1.9	1.9	-0.68	-0.84	35	16	6.6	0.4	6.3
15	inferior	849	0	0	16.9	16.9	0.19	0.25	2	5	0	0	0
	mid	720	0	0	17.8	14.5	-0.16	-0.22	3	9	0	0	0
	superior	571	0	0	16.3	13.4	-0.06	-0.17	3	9	0	0	0
16	inferior	1155	0	6	9.7	9.1	-0.25	-0.25	4	17	0	0	0
	mid	1135	0	0	11.2	6.0	-0.21	-0.18	4	4	0	0	0
	superior	1130	0	16	9.0	4.5	-0.41	-0.51	4	17	0	0	0
17	inferior	966	6	14	8.0	3.7	-0.39	-0.43	9	9	0	0	0
	mid	1053	50	34	3.6	2.3	-0.51	-0.49	29	31	0	0	0
	superior						excluded						
18	inferior	732	0	4	7.2	4.9	-0.36	-0.31	7	2	0	0	0
	mid	869	0	2	9.1	5.5	-0.32	-0.36	0	2	0	0	0
	superior						excluded						
19	inferior	1088	48	20	3.5	3.2	0.36	0.42	42	45	0	0	0
	mid	1067	14	12	8.1	6.8	0.10	0.23	12	10	0	0	0
	superior	974	24	50	8.0	6.9	-0.05	0.08	31	29	0	0	0
20	inferior	702	4	4	6.1	5.5	-0.11	-0.19	6	13	0	0	0
	mid	703	6	6	5.9	6.3	-0.44	-0.44	12	24	0	0	0
	superior	704	14	30	4.7	6.0	-0.66	-0.60	25	33	1.1	1.1	0
21	inferior	834	2	14	5.7	4.1	-0.24	-0.40	11	36	1.5	0	1.5
	mid	784	8	48	2.8	0.9	-0.65	-0.46	26	60	44.4	0	44.4
	superior	776	48	34	4.7	5.3	-0.32	-0.44	58	36	0	0	0
22	inferior	678	0	0	9.2	7.0	-0.12	-0.20	4	4	0	0	0
	mid	698	4	20	8.1	5.5	-0.47	-0.54	22	19	0	0	0
	superior	675	56	100	7.3	4.4	-0.69	-0.96	38	43	1.1	0.9	0.2
23	inferior	954	12	2	18.0	18.0	-0.07	-0.12	9	13	0	0	0
	mid	972	22	3	14.9	12.8	-0.26	-0.31	20	10	0	0	0
	superior	952	30	6	9.8	8.4	-0.35	-0.42	28	17	0	0	0
24	inferior	787	2	14	11.2	8.4	-0.22	-0.21	12	24	0	0	0

Supplemental Table 2. Individual results of electrophysiological parameters and epi-endocardial electrogram morphology (continued)

Patientno.	Location	SRCL (ms)	DA (mm)		Voltage (mV)		RS ratio		Fractionation (%)		EEA (%)	Epi delay (%)	Endo delay (%)
			Epi	Endo	Epi	Endo	Epi	Endo	Epi	Endo			
	mid	773	38	38	8.3	7.8	-0.11	-0.29	30	25	0	0	0
	superior						excluded						
25	inferior	728	72	32	3.7	2.8	-0.53	-0.60	45	37	0	0	0
	mid	770	60	22	4.7	4.4	-0.43	-0.25	23	5	7.2	7.2	0.0
	superior	750	50	34	5.2	3.8	-0.77	-0.56	39	40	16.1	15.1	1.0
26	inferior	802	20	24	11.5	10.7	-0.11	-0.16	19	18	0	0	0
	mid	800	26	32	9.5	6.8	-0.23	-0.22	28	31	0	0	0
	superior	794	14	48	7.7	6.2	-0.29	-0.40	28	38	0.6	0	0.6

SRCL = sinus rhythm cycle length; DA = delayed activation; EEA = endo-epicardial asynchrony.

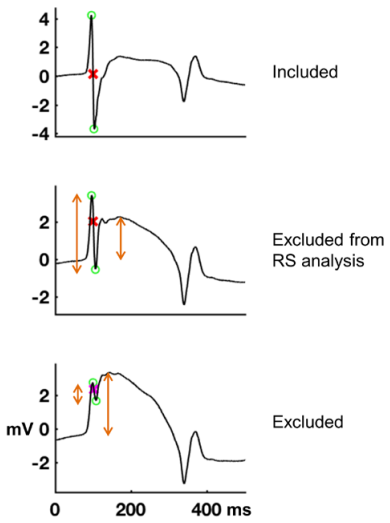

Supplemental Figure 1. Examples of potentials excluded from analysis.
The baseline after the potential in the middle is elevated > 1/3 of the total potential amplitude with a concordant shift of the potential to a positive dominance, this potential is excluded from RS analysis. The bottom potential is excluded from all analyses as the elevation of the baseline after the potential is larger than the total potential amplitude.

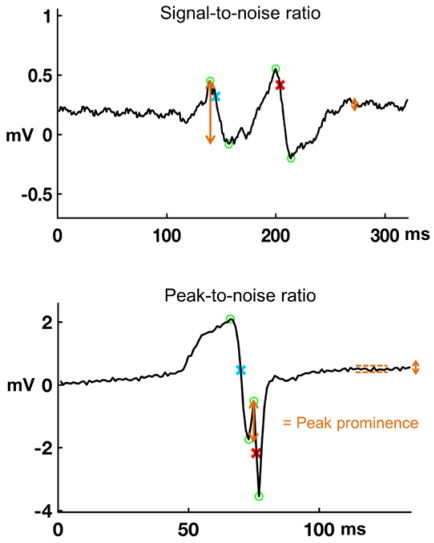

Supplemental Figure 2. Signal-to noise and peak-to-noise ratio.
Top: the ratio between the amplitude of the deflection and amplitude of the noise defined the signal-to-noise ratio. Bottom: the ratio between the peak prominence and the amplitude of the noise determined the detection of a new peak and the presence of a new deflection.

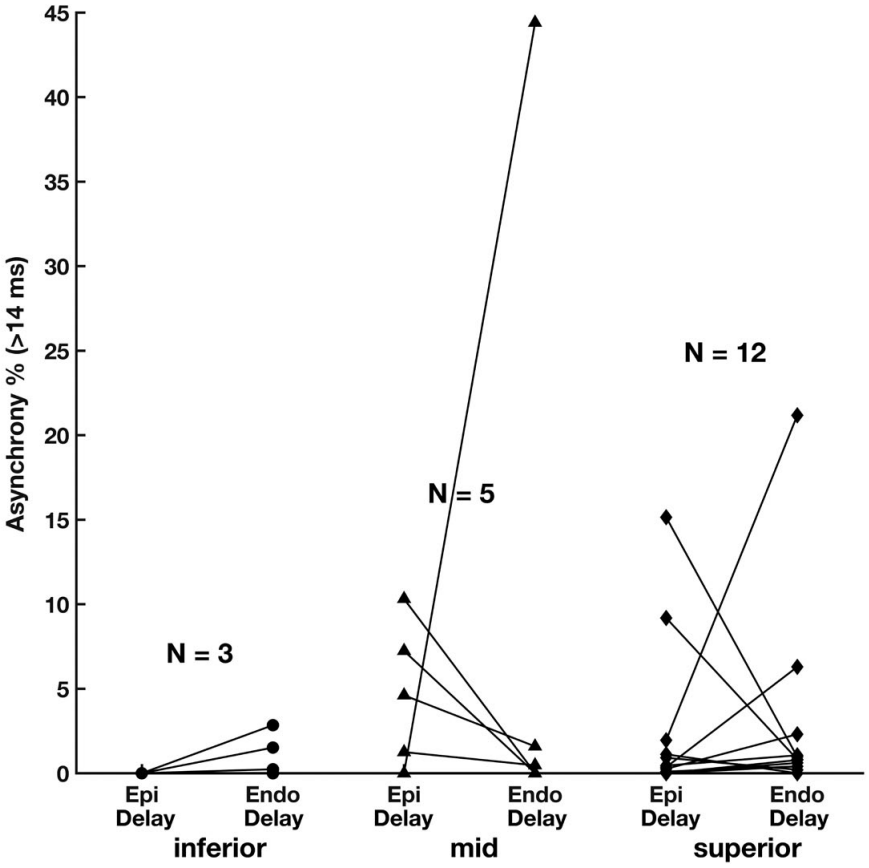

Supplemental Figure 3. Asynchrony in epi-endocardial activation.
Percentage of asynchrony (>14ms) with epicardial vs. endocardial delay per location for all patients with asynchrony. Asynchrony percentages are connected for each patient.